Switching intense laser pulses guided by Kerr-effect-modified modes of a hollow-core photonic-crystal fiber

D. A. Zheltikova,[1] M. Scalora,[2] A. M. Zheltikov,[1,3] M. J. Bloemer,[2] M. N. Shneider,[4] G. D'Aguanno,[2,5] and R. B. Miles[4]
[1]*Physics Department, M. V. Lomonosov Moscow State University, Moscow, 119992 Russia*
[2]*Weapons Sciences Directorate, U.S. Army Aviation and Missile Command, Huntsville, Alabama 35898-5000, USA*
[3]*International Laser Center, M. V. Lomonosov Moscow State University, Moscow, 119992 Russia*
[4]*Department of Mechanical and Aerospace Engineering, Princeton University, Princeton, New Jersey 08544-5263, USA*
[5]*Time Domain Corporation, Cummings Research Park, 7057 Old Madison Pike, Huntsville, Alabama 35806, USA*
(Received 12 March 2004; published 23 February 2005)

A Kerr-nonlinearity-induced profile of the refractive index in the hollow core of a photonic-crystal fiber (PCF) changes the spectrum of propagation constants of air-guided modes, effectively shifting the passbands in fiber transmission, controlled by the photonic band gaps (PBGs) of the cladding. This effect is shown to allow the creation of fiber switches for high-intensity laser pulses. The Kerr-nonlinearity control of air-guided modes in PCFs and the performance of a PCF switch are quantified by solving the propagation equation for the slowly varying envelope of a laser pulse guided in Kerr-effect-modified PCF modes. The spatial dynamics of the light field in a PBG waveguide switch is analyzed with the use of the slowly varying envelope approximation, demonstrating high contrasts of optical switching with PBG waveguides and hollow PCFs.

DOI: 10.1103/PhysRevE.71.026609 PACS number(s): 42.65.Wi

I. INTRODUCTION

Hollow-core fibers [1] have been shown to offer attractive solutions for the transport of intense laser radiation and enhanced nonlinear-optical interactions. This fiber design allows the sensitivity of nonlinear spectroscopy to be substantially improved [2,3] and extremely short pulses to be synthesized through Kerr-nonlinearity-induced self-phase-modulation [4,5], or high-order stimulated Raman scattering [6]. The magnitude of losses in standard, solid-cladding hollow fibers, however, scales [1] as λ^2/d^3 with the inner fiber diameter d and the radiation wavelength λ, which dictates the choice of hollow fibers with $d \sim 100-500$ μm for nonlinear-optical experiments. Such large-d fibers are essentially multimode, which limits their practical applications in ultrafast photonics.

Hollow-core photonic-crystal fibers (PCFs) [7,8] suggest the way to radically reduce the losses of air-guided modes. Such fibers guide light due to the high reflectivity of a two-dimensionally periodic (photonic-crystal) cladding (the inset in Fig. 1) within photonic band gaps (PBGs). Low-loss guiding (often in a single-mode regime) can be implemented under these conditions in a hollow core with a typical diameter of $10-20$ μm [7–9]. Hollow PCFs with such core diameters have been recently demonstrated to enhance nonlinear-optical processes, including stimulated Raman scattering [10], four-wave mixing [11], and self-phase-modulation [12]. Air-guided modes in hollow PCFs can support megawatt optical solitons [13] and allow transportation of high-intensity laser pulses for technological [14] and biomedical [15] applications.

Since the mechanism of waveguiding in hollow PCFs is based on PBGs, these fibers may allow interesting and practically useful fiber-optic extensions of all-optical signal processing concepts developed earlier for a variety of nonlinear periodic structures [16–19], including one-dimensional PBG structures [20–22]. A fiber-optic diode based on a combination of self-phase-modulation and filtering in air-guided modes of hollow PCFs and allowing optical processing and decoupling of high-intensity ultrashort laser pulses has been recently experimentally demonstrated by Konorov *et al.* [23].

In this work, we will show that the Kerr nonlinearity of the gas filling the hollow core of a PCF can be used to switch and control the transmission of intense laser pulses, as well as to perform logic operations on such pulses. It will be demonstrated that a Kerr-nonlinearity-induced profile of the refractive index in the hollow core of a PCF renormalizes the spectrum of propagation constants of air-guided modes, effectively shifting the passbands in fiber transmission, controlled by photonic band gaps of the cladding. We will solve the equation for the slowly varying envelope of a laser pulse guided in Kerr-effect-modified modes of a hollow PCF to assess the performance of such fiber switches.

II. GENERIC IDEA

The performance of a PCF switch, illustrated in Fig. 1, is based on the effective shift of passbands in fiber transmission due to Kerr-nonlinearity-induced changes in the propagation constants β of PCF modes. The passbands in the transmission of a PCF (the inset in Fig. 2) are maps of the photonic band gaps of the fiber cladding (shaded areas in Fig. 1). This mapping is defined [7,24] by crossings of dispersion lines of air-guided PCF modes with PBGs (Fig. 1). Changes in the dispersion of air-guided modes would, therefore, correspond to variations in the transmission of a PCF at a given frequency.

We assume that the frequency of a pump pulse ω_p is tuned to the center of the passband in the transmission of the PCF related to the PBG of the cladding shown by shaded area 1 in Fig. 1. The frequency of the probe pulse is chosen close to an edge of a passband corresponding to the fundamental (solid

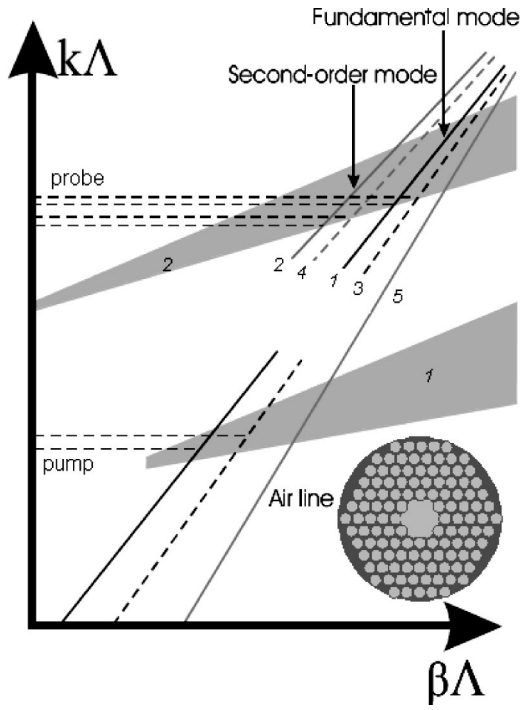

FIG. 1. Performance of a PCF switch, shown in the $\beta\Lambda$-$k\Lambda$ diagram [24] of the fiber. Lines 1–4 represent the dispersion of the fundamental (1, 3) and higher-order (2, 4) air-guided modes in an unperturbed hollow-core PCF (1, 2) and a PCF with a refractive index profile modified by a pump pulse (3, 4). Line 5 displays the dispersion of the gas filling the fiber core (atmospheric air). Shaded areas 1 and 2 correspond to photonic band gaps of the PCF cladding. The inset sketches the cross-section view of a hollow-core photonic-crystal fiber.

line 1 in Fig. 1) or one of the higher-order (solid line 2) air-guided modes of the hollow PCF. As the pump pulse propagates through the PCF, it induces intensity-dependent changes in the refractive index of the gas filling the fiber core and the material of the fiber cladding. This change in the refractive index shifts dispersion curves in the $\beta\Lambda$-$k\Lambda$ diagram of Fig. 1 ($k=\omega/c$ is the wave number, c is the speed of light, and Λ is the period of the photonic-crystal structure in the fiber cladding). If the nonlinear refractive indices of the gas and the material of the fiber cladding are positive, the probe pulse effectively sees the passband blueshifted (the shifted dispersion curves for the fundamental and higher-order air-guided modes of the PCF are shown by dashed lines 3 and 4, respectively). The transmission of the probe pulse is reduced in such a situation.

Transmission variation of the opposite sign can be achieved at the frequency of the probe pulse by choosing this frequency outside the passband and shifting the passband toward this frequency with the use of the Kerr effect. In the following sections of this paper, we will quantify the performance of the PCF switch by estimating changes in propagation constants attainable with typical parameters of laser pulses and solving the equation for the slowly varying amplitude of the probe pulse in Kerr-effect-modified modes of a hollow PCF.

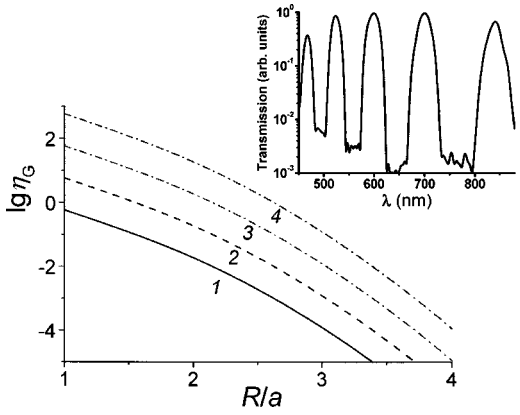

FIG. 2. The factor η_G, quantifying the ratio of the contributions of the fiber core and the fiber cladding to the nonlinear-optical variation of propagation constants, as a function of the ratio of the fiber core radius R to the effective mode radius $a=a_n=a_m$ for a Gaussian model of field intensity distribution in PCF modes [Eq. (7)] with $\bar{n}_2/n_2=1$ (line 1), 10 (line 2), 100 (line 3), and 1000 (line 4). The inset shows a typical wavelength dependence of transmission for a hollow-core photonic-crystal fiber (adapted from [28]).

III. KERR-NONLINEARITY CONTROL OF THE DISPERSION OF PCF MODES

The Kerr effect [25] induced by intense laser radiation guided in the modes of a hollow-core PCF gives rise to a nonuniform, intensity-dependent addition $\delta n(r)$ to the refractive index n_0 of the gas filling the PCF core, modifying the profile of the refractive index in the fiber,

$$n(r) = n_0 + \delta n(r). \tag{1}$$

The modified refractive-index profile is determined by the profile of radiation intensity $I(r)$ and the nonlinear refractive index $\tilde{n}_2$:

$$\delta n(r) = \tilde{n}_2 I(r). \tag{2}$$

A small variation in the refractive index δn renormalizes the spectrum of PCF eigenvalues, changing the propagation constants β_i of air-guided modes. The reciprocity theorem for optical waveguides [26] gives the following expression for the correction to the propagation constant of a guided mode in an arbitrary fiber with a small perturbation of the refractive index $\delta n(r)$:

$$\delta\beta \approx k\frac{\int_A \delta n(r)\Psi^2 dA}{\int_A \Psi^2 dA}, \tag{3}$$

where Ψ is the guided mode in an unperturbed fiber and A is the cross section of the fiber.

We can adapt this result to a hollow PCF with a Kerr-effect-induced variation in the refractive index, given by Eq. (2), rewriting Eq. (3) as

$$\delta\beta \approx kI_0 \frac{\int_0^\infty \tilde{n}_2 |f_n(r)|^2 |f_m(r)|^2 r\, dr}{\int_0^\infty |f_m(r)|^2 r\, dr}, \tag{4}$$

where I_0 is the peak intensity in the PCF mode guiding the pump pulse and $f_n(r)$ and $f_m(r)$ are the functions describing the field distribution in the PCF modes guiding the pump and probe pulse, respectively.

Both the fiber core and the fiber cladding can generally contribute to $\delta\beta$. Since the nonlinear refractive index of the PCF cladding, $\overline{n_2}$, is typically higher than the nonlinear refractive index n_2 of the gas filling the hollow core, it is instructive to estimate the ratio

$$\eta = \frac{\overline{n_2}}{n_2} \frac{\int_R^\infty |f_n(r)|^2 |f_m(r)|^2 r\, dr}{\int_0^R |f_n(r)|^2 |f_m(r)|^2 r\, dr} \tag{5}$$

(R is the core radius), quantifying the relation between the contributions of the fiber core and the fiber cladding to the nonlinear-optical variation of propagation constants. With a simple Gaussian model of field intensity distribution in PCF modes,

$$|f_n(r)| \propto \exp\left(-\frac{r^2}{a_n^2}\right), \tag{6}$$

where a_n is the effective mode radius, the integration in Eq. (5) yields

$$\eta_G = \frac{\overline{n_2}}{n_2} \frac{1}{\exp[2R^2(a_n^{-2} + a_m^{-2})] - 1}. \tag{7}$$

As can be seen from Eq. (7), the contribution of the PCF cladding to the variation of propagation constants rapidly decays with the growth in the degree of field confinement in the fiber core, quantified by the ratio $R/a_{n,m}$ (Fig. 2). Therefore, even though the nonlinearity of the PCF cladding is typically much higher than the nonlinearity of the gas filling the fiber core, the contribution of the fiber cladding to variations of propagation constants of well-localized fiber modes can be neglected. Corrections $\delta\beta$ for such modes in the approximation of a Gaussian field distribution [Eq. (6)] are then estimated as

$$\delta\beta \approx kI_0 n_2 \frac{a_m^2}{a_m^2 + a_n^2}. \tag{8}$$

In the following section, we will substitute Eq. (8) into the equation governing the evolution of a laser pulse propagating through a hollow PCF to demonstrate the switching function of such a fiber due to the Kerr-nonlinearity-induced change in propagation constants.

IV. EVOLUTION OF A LASER PULSE GUIDED THROUGH A HOLLOW PCF

We now apply a standard approach of the slowly varying envelope approximation to describe the propagation of a laser pulse through a hollow-core PCF filled with a gas with a Kerr nonlinearity. The equation for the pulse envelope A is written as [25,27]

$$i\frac{\partial A}{\partial z} = -\frac{i}{2}\alpha A - \gamma |A|^2 A, \tag{9}$$

where α is the magnitude of losses and γ is the nonlinear coefficient responsible for self-phase-modulation.

Unlike the elementary theory of self-phase-modulation, the magnitude of losses α, appearing in Eq. (9), is a function of the intensity of the pump pulse. To find this intensity dependence of losses, which is at the heart of the operation of the PCF switch, we expand α as a Taylor series in a small variation of the propagation constant $\delta\beta$:

$$\alpha \approx \alpha_0 + \delta\alpha, \tag{10}$$

with

$$\delta\alpha \approx \frac{c}{n_{\text{eff}}} \frac{\partial\alpha}{\partial\omega} \delta\beta, \tag{11}$$

where n_{eff} is the effective refractive index of the guided mode.

Using Eq. (8), we find that

$$\delta\alpha \approx kI_0 n_2 \frac{c}{n_{\text{eff}}} \frac{\partial\alpha}{\partial\omega} \xi, \tag{12}$$

where

$$\xi = \frac{\int_0^\infty |f_n(r)|^2 |f_m(r)|^2 r\, dr}{\int_0^\infty |f_m(r)|^2 r\, dr}. \tag{13}$$

Substituting Eqs. (10) and (12) into Eq. (9), we derive the following propagation equation:

$$2i\frac{\partial A}{\partial z} + i\alpha_0 A + 2k\frac{\vartheta_2}{n_0}\left(1 + i\frac{c}{2n_{\text{eff}}}\frac{\partial\alpha}{\partial\omega}\xi\right)A|A|^2 = 0, \tag{14}$$

where $\vartheta_2 |A|^2 = n_2 I$.

With the field $E(l)$ at the output of a fiber with a length l related to the input field $E(0)$ by $E(l) = a\exp(i\varphi)E(0)$, where φ is the phase shift, Eq. (14) gives the following analytic solution for a:

$$a^2 = \frac{\exp(-\alpha_0 l)}{1 - \frac{\lambda}{n_{\text{eff}}}\frac{\partial\alpha}{\partial\lambda} n_2 \xi I_0 L_{\text{eff}}}, \tag{15}$$

where λ is the radiation wavelength and

$$L_{\text{eff}} = [1 - \exp(-\alpha_0 l)]/\alpha_0. \tag{16}$$

Expression (15) serves to illustrate the operation of the PCF switch. As long as the second, nonlinear term in the

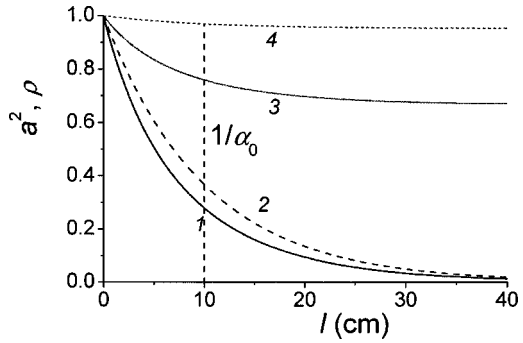

FIG. 3. Parameters a^2 (curves 1 and 2) and ρ (curves 3 and 4) calculated as functions of the fiber length l in accordance with Eqs. (15) and (17), respectively, in the absence of the pump pulse (curve 1) and in the presence of a pump pulse with the intensity $I_0 = 10^{14}$ W/cm^2 (lines 2–4) for $n_2 = 5 \times 10^{-19}$ cm^2/W (atmospheric air), $\alpha_0 = 0.1$ cm^{-1}, and $\partial\alpha/\partial\lambda = 10^7$ cm^{-2} (lines 2 and 3) and 10^6 cm^{-2} (line 4). The dotted line corresponds to the PCF length $l = 1/\alpha_0$.

denominator of a^2 is small compared to unity, no switching is achieved. The nonlinear term is controlled by the peak intensity of the pump pulse, I_0; the nonlinear refractive index of the gas filling the fiber core, n_2; overlapping of the modes guiding the pump and probe pulses, ξ; the propagation length l; and the gradient of PCF transmission at the wavelength of the probe pulse, $\partial\alpha/\partial\lambda$ (or $\partial\alpha/\partial\omega$).

The ratio of the intensities of the probe signal at the output of the PCF in the presence and in the absence of the pump field can be used as a measure of the switching contrast. Using Eq. (15), we can represent this ratio as

$$\rho = \frac{1}{1 - \dfrac{\lambda}{n_{\text{eff}}}\dfrac{\partial\alpha}{\partial\lambda} n_2 \xi I_0 L_{\text{eff}}}. \tag{17}$$

The effective length L_{eff}, as can be seen from Eq. (16), is limited, tending to $1/\alpha_0$ for large l. Such a behavior of L_{eff} dictates the choice of the optimal propagation length for a reasonable compromise between the switching contrast and the amplitude of the output signal, which decays as a function of the propagation length l (Fig. 3). Setting $L_{\text{eff}} = 1/\alpha_0$ in Eq. (17) (the dotted line in Fig. 3), we thus find the limiting value of the ratio ρ (Fig. 3):

$$\rho_{\text{lim}} = \frac{1}{1 - \dfrac{\lambda}{n_{\text{eff}}}\dfrac{\partial\alpha}{\partial\lambda}\dfrac{n_2 \xi I_0}{\alpha_0}}. \tag{18}$$

The derivative $\partial\alpha/\partial\lambda$, characterizing the sharpness of the PCF passband, is determined by the structure of the fiber. Calculations presented in [28] demonstrate that the values of $|\partial\alpha/\partial\lambda|$ on the order of 10^7 cm^{-2} can be achieved for hollow-core waveguides with a coaxial periodic cladding (hollow Bragg waveguides) with a properly chosen air-filling fraction of the cladding. Such values of $|\partial\alpha/\partial\lambda|$ correspond to the limiting switching contrast $\sigma_{\text{lim}} = 1/\rho_{\text{lim}}$ of about 1.5 for a 20-cm PCF and the pump intensity of 10^{14} W/cm^2 (curve 3 in Fig. 3). In Fig. 2, we plot a typical transmission characteristic for a hollow PCF with a period of the cladding of about 5 μm and a core diameter of about 14 μm, measured by Konorov *et al.* [28]. With an estimate $|\partial\alpha/\partial\lambda| \sim 10^6$ cm^{-2} obtained from this plot, we arrive at a limiting switching contrast σ_{lim} of about 1.05 for a 20-cm PCF and the pump intensity of 10^{14} W/cm^2 (curve 4 in Fig. 3). Requirements for the pump intensity can be substantially loosened by using gases with higher (e.g., resonant) nonlinearities.

The estimates presented above show that the Kerr effect in hollow PCFs may provide sufficiently high contrasts of switching. The switching efficiency can be further improved by increasing the pressure of the gas filling the fiber core. Analysis of nonlinear-optical interactions of short laser pulses in the regime of high pressures should, however, include ionization effects, which may have a noticeable influence on the properties of air-guided modes in PCFs at high laser intensities. Intense ultrashort pump pulses, on the other hand, may open an additional channel for the switching of a probe pulse. The spectral width of the probe pulse induced by cross-phase modulation may become comparable in this regime with the width of the passband in PCF transmission. The losses of the probe pulse can be then controlled by varying the intensity of the pump field, suggesting a method of switching competitive in its efficiency with the mechanism considered in this work.

V. SPATIAL DYNAMICS OF THE LIGHT FIELD IN A PBG WAVEGUIDE SWITCH

In this section, we use the standard slowly varying envelope approximation (SVEA) [25] to examine the influence of the Kerr-nonlinearity-induced change in the refractive index in the hollow core of a PCF on the spatial dynamics of air-guided modes propagating through such a fiber. A hollow PCF will be modeled in our numerical simulations as a coaxial periodic (Bragg) hollow waveguide [29–33]. The transverse profile of the refractive index in such a waveguide is shown in Fig. 4. The spatially periodic modulation of the refractive index in the cladding gives rise to photonic band gaps, which can support, similar to the case of a hollow PCF, air-guided modes in the hollow core of the waveguide. Since PBG shifting is at the heart of our PCF switch (Fig. 1), analysis of a coaxial hollow waveguide is very instructive for a qualitative understanding of the switching abilities and physical limitations of hollow PCFs. This analysis will also serve to demonstrate the potential of coaxial Bragg waveguides [29,30] for the creation of PBG switches. Finally, the model of a waveguide with a periodic cladding considered in this section is applicable to the analysis of planar waveguides with a periodically modulated refractive index of the cladding, similar to waveguides demonstrated by Yeh and Yariv [34,35]. Our concept of a PBG switch can be thus extended to include the planar waveguide geometry.

We start with a standard SVEA equation adapted to describe the propagation of TE modes in a coaxial or slab waveguide with a PBG cladding:

$$2ik\frac{\partial E}{\partial z} = -\left[k^2 - \frac{\omega^2}{c^2}n^2(x)\right]E - \frac{\partial^2 E}{\partial x^2} - 4\pi\frac{\omega^2}{c^2}P_{\text{NL}}. \tag{19}$$

Here, z and x are the longitudinal and transverse coordinates, respectively, $n(x)$ is the transverse profile of the refractive

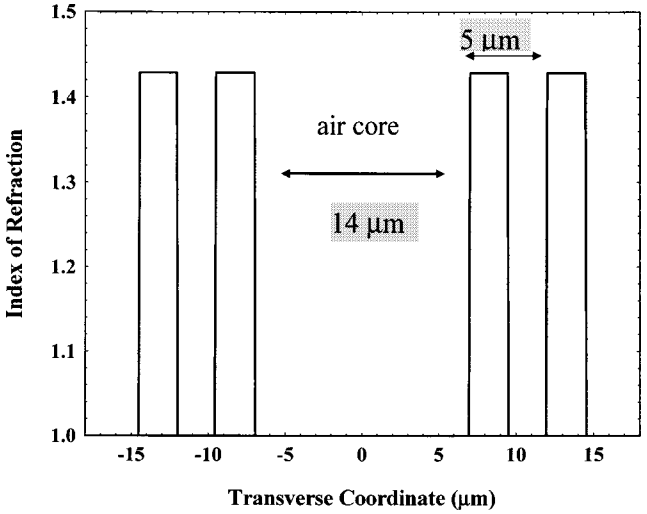

FIG. 4. Transverse profile of the refractive index in a hollow coaxial waveguide.

index (Fig. 4), $k=\omega/c$, and $P_{\mathrm{NL}}=\chi^{(3)}|E|^2E$ is the nonlinear polarization. Introducing the longitudinal and transverse dimensionless coordinates $\xi=z/\lambda_0$ and $\tilde{x}=x/\lambda_0$, where λ_0 is an arbitrary reference wavelength that represents the spatial scale of the problem, we can write

$$\frac{\partial E}{\partial \xi} = i\pi[n^2(x)-1]\frac{\lambda_0}{\lambda_{\mathrm{in}}}E + \frac{i}{4\pi}\frac{\lambda_0}{\lambda_{\mathrm{in}}}\frac{\partial^2 E}{\partial x^2} + i4\pi^2\frac{\lambda_0}{\lambda_{\mathrm{in}}}\chi^{(3)}|E|^2E, \tag{20}$$

where λ_{in} is the wavelength of incident radiation, and $\tilde{\lambda}=\lambda_{\mathrm{in}}/\lambda_0$ is the scaled incident wavelength.

Generally, Eq. (20) allows us to simulate the spatial dynamics of arbitrary input field profiles in a waveguide with an arbitrary, one-dimensional transverse index profile. To illustrate the switching behavior of modes in a guiding layer or a fiber core with a Kerr nonlinearity, we choose a simple symmetric structure, composed of an air core and two coaxial cylinders, as depicted in Fig. 4. Since we are using dimensionless coordinates, the results of this analysis can be scaled up or down the spectrum, allowing the description of PBG waveguides with other dimensions by simply changing the parameter λ_0. We chose $\lambda_0=1$ μm for our calculations. Changing the layer or core thickness generally produces no qualitative changes to the transmission profile, except for a blue- or redshift of the band structure, and an increase or a decrease in the number of passbands and gaps within a specified range. In Fig. 5(a) we show the linear band structure which comes as a result of integrating Eq. (20), for a waveguide with a 14-μm core, and coaxial cylinder with 5-μm periods. A number of gaps and passbands are clearly visible, and these basic features are shared by all similar devices.

In what follows, we will examine the afore mentioned waveguide with a 14-μm core diameter and two coaxial cylinders with a period of 5 μm, as shown in Fig. 4, for a structure with an overall size of 29 μm, and a length of 0.5 cm. The solid lines with open circles in Figs. 5(a) and 5(b) show the linear transmittance (i.e., $\chi^{(3)}|E|^2=0$) of this

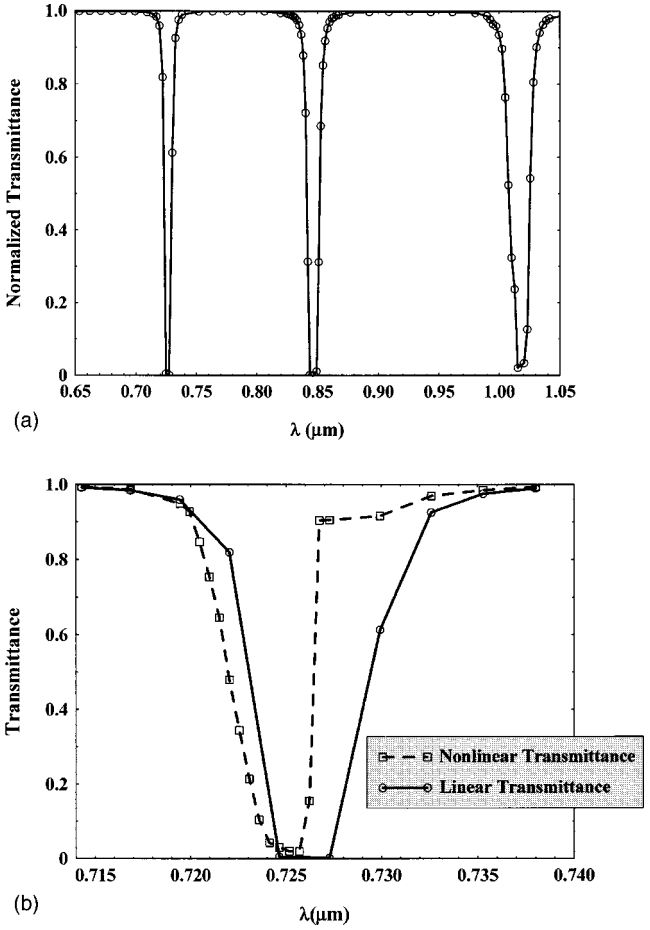

FIG. 5. Normalized transmittance of the hollow PBG waveguide in the linear regime, $\chi^{(3)}|E|^2=0$ [open circles in both (a) and (b)] and in the nonlinear regime, $\chi^{(3)}|E|^2\sim 4\times 10^{-4}$ (squares); (a) several passbands are shown and (b) close-up of the spectral range around the band edge.

guide, while the dashed curve with open squares in Fig. 5(b) shows the transmittance in the nonlinear regime with $\chi^{(3)}|E|^2\sim 4\times 10^{-4}$. The nonlinear index of refraction, which can be induced, for example, by a high-power pump pulse, leads to an overall shift of the passbands, switching cw radiation. In the dynamic regime, this effect gives rise to a reversible shift, probed by field wave forms with a time-dependent intensity. This situation is ideally suited for optical self-limiting of laser pulses.

The band edge around 725 nm shifts by approximately 8 nm in the nonlinear regime [cf. the lines with circles and squares in Figs. 5(a) and 5(b)]. This result, in fact, suggests that laser radiation with a wavelength tuned near 725 nm can be switched on by increasing its intensity in such a way as to approximately satisfy the condition $\chi^{(3)}|E|^2\sim 4\times 10^{-4}$. In a pump-probe arrangement, a control (pump) beam can be used to switch a probe beam on or off. A similar dynamics was predicted in the context of a photonic band edge optical limiter and switch [20].

The switching of a laser beam propagating through the PBG waveguide is illustrated in Figs. 6 and 7. In Fig. 6, we plot the radiation energy in the PBG waveguide as a function of propagation distance for a low-intensity beam (circles)

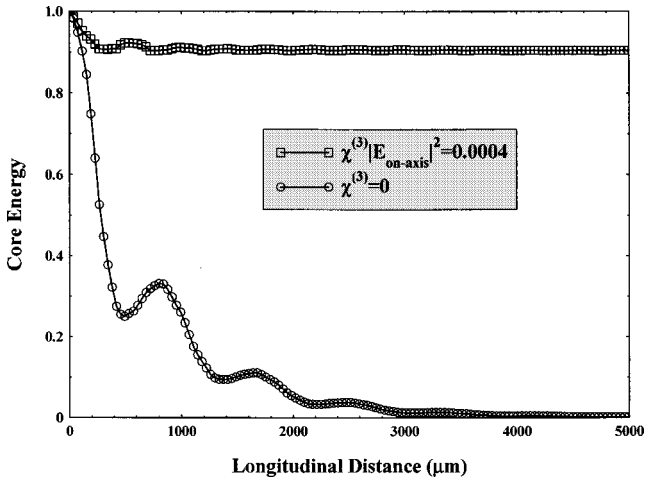

FIG. 6. The radiation energy in the PBG waveguide (in arbitrary units) as a function of propagation distance for a low-intensity radiation field with $\chi^{(3)}|E|^2=0$ and a central wavelength of 725 nm (circles) and a high-intensity radiation field with $\chi^{(3)}|E|^2\sim 4\times 10^{-4}$ tuned at the same wavelength (squares).

tuned at 725 nm, thus falling outside the passband in fiber transmission, and a high-intensity beam tuned at the same wavelength (squares). The contrast in output energy between the two regimes is approximately two orders of magnitude for a section of a waveguide with a length of 0.5 cm. The switching length is thus shown to be several orders of magnitude less than the typical attenuation length for hollow PCFs. With losses as low as 13 dB/km recently reported for hollow PCFs [8], attenuation should not lead to serious problems for switching applications, where only a few centimeters of PCF is necessary. The spatial dynamics of the radiation field propagating in the hollow PBG waveguide is shown in Figs. 7(a) and 7(b). In Fig. 7(a), the laser radiation rapidly leaks into the cladding, leaving the guiding layer and leading to a low level of output signal (circles in Fig. 6). In the nonlinear regime [Fig. 7(b)], the field is guided with much lower losses, resulting in a substantially higher level of output signal (squares in Fig. 6). Numerical simulations thus demonstrate optical switching in hollow PCFs with a contrast of "on" and "off" states reaching two orders of magnitude for properly designed fibers. The passband shift, underlying switching in hollow PCFs, is controlled by the intensity of the laser field and is independent of the phase of this field. The switching performance of PCFs is, therefore, insensitive to the phase matching of the pump and probe fields.

PCF switches demonstrated in this work not only offer practically advantageous fiber-optic extensions of the generic PBG switching concept, but also offer a unique possibility to control and manipulate isolated waveguide modes of high-intensity laser fields. Unlike conventional fiber-Bragg-grating photonic components and solid-state PBG switches, hollow PCFs can guide light fields in the gas phase, allowing the field intensity to be substantially increased with no damage on the fiber. While standard, solid-cladding hollow fibers can efficiently guide light only in the multimode regime (with their losses scaling as λ^2/d^3 with the inner fiber diameter d and the radiation wavelength λ [1]), hollow PCFs can

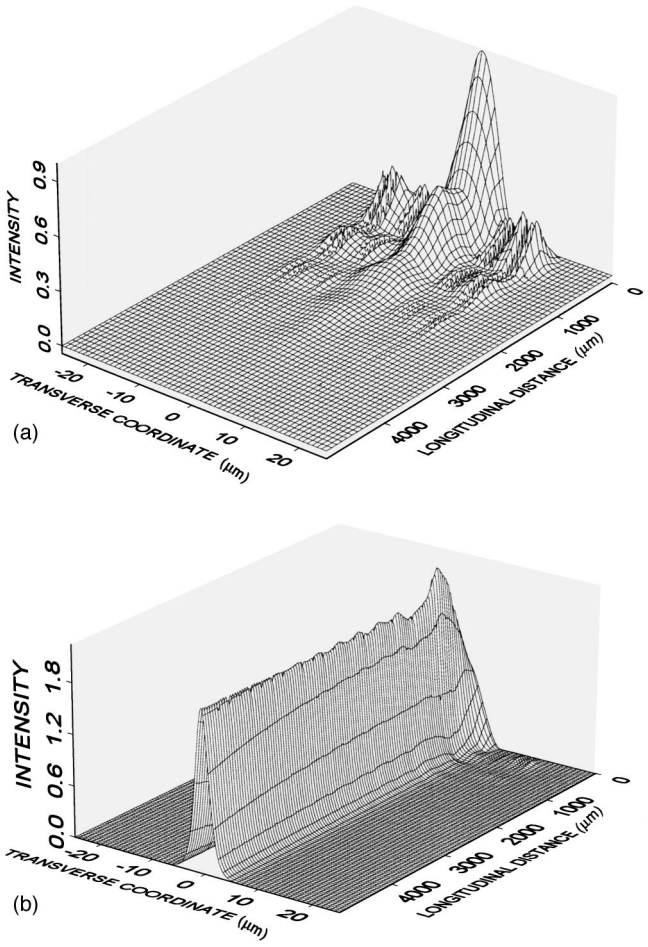

FIG. 7. The spatial dynamics of the radiation field in the hollow PBG waveguide: $\chi^{(3)}|E|^2=0$ (a) and (b) $\sim 4\times 10^{-4}$. The transverse and longitudinal coordinates are defined as $\tilde{x}=x/\lambda_0$ and $\xi=z/\lambda_0$, respectively. Radiation intensity is given in arbitrary units. We assume that the radiation is absorbed once it leaves the PBG guide.

support isolated guided modes of high-intensity light fields, making these modes switchable and controllable through the nonlinear shift of photonic band gaps of the fiber cladding.

VI. CONCLUSION

We have shown in this work that a Kerr-nonlinearity-induced profile of the refractive index in the hollow core of a photonic-crystal fiber changes the spectrum of propagation constants of air-guided modes, effectively shifting the passbands in fiber transmission, controlled by photonic band gaps of the cladding. This effect is shown to allow the creation of fiber switches, processors, and logic gates for high-intensity laser pulses. We have quantified the Kerr-nonlinearity control of air-guided modes in PCFs and the performance of a PCF switch by solving the propagation equation for the slowly varying envelope of a laser pulse guided in PCF modes modified by a pump pulse through the Kerr nonlinearity of the gas filling the fiber core. Numerical SVEA analysis of the spatial dynamics of the light field in a PBG waveguide switch suggests ways to achieve high contrasts of optical

switching with PBG waveguides and hollow PCFs. Using Kerr nonlinearity is only one of the methods to modify the dispersion of air-guided modes in PCFs. Ionization-induced changes in the refractive index profile, for example, would result in an effective redshifting of PCF passbands.

ACKNOWLEDGMENTS

We are grateful to S. O. Konorov, A. B. Fedotov, and D. A. Sidorov-Biryukov for useful discussions. This study was supported in part by the President of Russian Federation Grant No. MD-42.2003.02, the Russian Foundation for Basic Research (Projects No. 03-02-16929, No. 04-02-81036-Bel2004-a, and No. 03-02-20002-BNTS-a), and INTAS (Projects No. 03-51-5037 and No. 03-51-5288). The research described in this publication was made possible in part by Award No. RP2-2558 of the U.S. Civilian Research & Development Foundation for the Independent States of the Former Soviet Union (CRDF). This material is also based upon work supported by the European Research Office of the U.S. Army under Contract No. 62558-04-P-6043.

[1] E. A. J. Marcatili and R. A. Schmeltzer, Bell Syst. Tech. J. **43**, 1783 (1964).
[2] R. B. Miles, G. Laufer, and G. C. Bjorklund, Appl. Phys. Lett. **30**, 417 (1977).
[3] A. B. Fedotov, F. Giammanco, A. N. Naumov, P. Marsili, A. Ruffini, D. A. Sidorov-Biryukov, and A. M. Zheltikov, Appl. Phys. B: Lasers Opt. **72**, 575 (2001).
[4] M. Nisoli, S. De Silvestri, and O. Svelto, Appl. Phys. Lett. **68**, 2793 (1996).
[5] M. Nisoli, S. De Silvestri, O. Svelto, R. Szipöcs, K. Ferencz, Ch. Spielmann, S. Sartania, and F. Krausz, Opt. Lett. **22**, 522 (1997).
[6] N. Zhavoronkov and G. Korn, Phys. Rev. Lett. **88**, 203901 (2002).
[7] R. F. Cregan, B. J. Mangan, J. C. Knight, T. A. Birks, P. St. J. Russell, P. J. Roberts, and D. C. Allan, Science **285**, 1537 (1999).
[8] P. St. J. Russell, Science **299**, 358 (2003).
[9] S. O. Konorov, A. B. Fedotov, O. A. Kolevatova, V. I. Beloglazov, N. B. Skibina, A. V. Shcherbakov, and A. M. Zheltikov, JETP Lett. **76**, 341 (2002).
[10] F. Benabid, J. C. Knight, G. Antonopoulos, and P. St. J. Russell, Science **298**, 399 (2002).
[11] S. O. Konorov, A. B. Fedotov, and A. M. Zheltikov, Opt. Lett. **28**, 1448 (2003).
[12] S. O. Konorov, D. A. Sidorov-Biryukov, I. Bugar, D. Chorvat, Jr., V. I. Beloglazov, N. B. Skibina, A. V. Shcherbakov, D. Chorvat, and A. M. Zheltikov, Quantum Electron. **34**, 56 (2004).
[13] D. G. Ouzounov, F. R. Ahmad, D. Müller, N. Venkataraman, M. T. Gallagher, M. G. Thomas, J. Silcox, K. W. Koch, and A. L. Gaeta, Science **301**, 1702 (2003).
[14] S. O. Konorov, A. B. Fedotov, O. A. Kolevatova, V. I. Beloglazov, N. B. Skibina, A. V. Shcherbakov, E. Wintner, and A. M. Zheltikov, J. Phys. D **36**, 1375 (2003).
[15] S. O. Konorov, A. B. Fedotov, V. P. Mitrokhin, V. I. Beloglazov, N. B. Skibina, A. V. Shcherbakov, E. Wintner, M. Scalora, and A. M. Zheltikov, Appl. Opt. **43**, 2251 (2004).
[16] C. M. de Sterke and J. E. Sipe, Prog. Opt. **33**, 203 (1994).
[17] B. J. Eggleton, R. E. Slusher, C. M. de Sterke, P. A. Krug, and J. E. Sipe, Phys. Rev. Lett. **76**, 1627 (1996).
[18] N. G. R. Broderick, D. Taverner, and D. J. Richardson, Opt. Express **3**, 447 (1998).
[19] N. D. Sankey, D. F. Prelewitz, and T. G. Brown, Appl. Phys. Lett. **60**, 1427 (1992).
[20] M. Scalora, J. P. Dowling, C. M. Bowden, and M. J. Bloemer, Phys. Rev. Lett. **73**, 1368 (1994).
[21] M. D. Tocci, M. J. Bloemer, M. Scalora, J. P. Dowling, and C. M. Bowden, Appl. Phys. Lett. **66**, 2324 (1995).
[22] B. Y. Soon, J. W. Haus, M. Scalora, and C. Sibilia, Opt. Express **11**, 2007 (2003).
[23] S. O. Konorov, D. A. Sidorov-Biryukov, I. Bugar, M. J. Bloemer, V. I. Beloglazov, N. B. Skibina, D. Chorvat, Jr., D. Chorvat, M. Scalora, and A. M. Zheltikov, Appl. Phys. B: Lasers Opt. **78**, 547 (2004).
[24] J. Broeng, S. E. Barkou, T. Søndergaard, and A. Bjarklev, Opt. Lett. **25**, 96 (2000).
[25] Y. R. Shen, *The Principles of Nonlinear Optics* (Wiley, New York, 1984).
[26] A. W. Snyder and J. D. Love, *Optical Waveguide Theory* (Chapman and Hall, New York, 1983).
[27] G. P. Agrawal, *Nonlinear Fiber Optics* (Academic, Boston, 1989).
[28] S. O. Konorov, O. A. Kolevatova, A. B. Fedotov, E. E. Serebryannikov, D. A. Sidorov-Biryukov, J. M. Mikhailova, A. N. Naumov, V. I. Beloglazov, N. B. Skibina, L. A. Mel'nikov, A. V. Shcherbakov, and A. M. Zheltikov, JETP **96**, 857 (2003).
[29] M. Ibanescu, Y. Fink, S. Fan, E. L. Thomas, and J. D. Joannopoulos, Science **289**, 415 (2000).
[30] S. G. Johnson, M. Ibanescu, M. Skorobogatiy, O. Weisberg, T. D. Engeness, M. Soljacic, S. A. Jacobs, J. D. Joannopoulos, and Y. Fink, Opt. Express **9**, 748 (2001).
[31] P. Yeh, A. Yariv, and E. Marom, J. Opt. Soc. Am. **68**, 1196 (1978).
[32] Yong Xu, R. K. Lee, and A. Yariv, Opt. Lett. **25**, 1756 (2000).
[33] G. Ouyang, Yong Xu, and A. Yariv, Opt. Express **9**, 733 (2001).
[34] P. Yeh and A. Yariv, Opt. Commun. **19**, 427 (1976).
[35] A. Yariv and P. Yeh, *Optical Waves in Crystals* (Wiley, New York, 1984).